Determining the Structure of Phosphorus in Phase IV

Takahiro Ishikawa,* Hitose Nagara,† Koichi Kusakabe,‡ and Naoshi Suzuki§

Division of Frontier Materials Science, Graduate School of Engineering Science, Osaka University, Toyonaka, Osaka 560-8531, Japan

(Received 10 September 2005; published 8 March 2006)

We explore the unknown structure of phosphorus in phase IV (P-IV phase) based on first-principles calculations using the metadynamics simulation method. Starting from the simple cubic structure, we find a new modulated structure of the monoclinic lattice. The modulation is crucial to the stability of the structure. Through refining the structure further by changing the modulation period, we find the structure whose x-ray powder diffraction pattern is in best agreement with the experimental pattern. We expect that the modulation period of the structure in the P-IV phase is very close to that found in this study and probably incommensurate.

DOI: 10.1103/PhysRevLett.96.095502 PACS numbers: 61.50.Ah, 62.50.+p, 64.70.Kb

Recent progress in high-pressure physics has enhanced our recognition of a wide variety of crystal structures. Development of high-pressure techniques has also enabled the identification of structures that are stabilized only in a narrow pressure range. Interesting structures were found unexpectedly through high-pressure experiments. For instance, modulated structures are often found in the high-pressure phases of elements. Lattice modulations have been found in group Vb elements, including As, Sb, and Bi [1,2], and the group VIb elements S [3], Se [4], and Te [5]. Modulated structures have also been reported in the halogens I [6] and Br [7].

Scarcity of experimental ultrahigh-pressure data restricts high-pressure studies. Thus, researchers often encounter difficulties in the identification of a crystal structure on the basis of experimental data alone. A theoretical approach provides additional information on the same problem. First-principles theory for determining crystal structures is believed to be sufficiently accurate. However, the limitations of computational resources sometimes impede full structure searches.

We will focus on the case of phase IV of the phosphorus (P-IV) phase. Observation of the P-IV phase was first reported by Akahama *et al.* [8] in 1999. In the sequence of pressure-induced transformations, the simple cubic (sc) phase (P-III) appears at 10 GPa at low temperature. Akahama *et al.* [8] reported the appearance of a simple hexagonal (sh) phase, i.e., the P-V phase, which stabilizes above 137 GPa, and an intermediate phase, i.e., the P-IV phase, between sc and sh on the basis of x-ray diffraction data. At even higher pressures, the bcc structure (P-VI) has been theoretically predicted [9] and later identified in an experiment at 262 GPa [10]. The structure of phase IV, however, has not been identified experimentally. Ordinary Rietveld analysis based on a knowledge of the monoclinic symmetry alone has not been successful, presumably owing to the complexity of the lattice. Thus, we must guess the crystal structure or a pseudocrystal.

Several structures have been tested as candidate structures for P-IV. Ahuja considered a structure of space group *Imma* [11]. Ehlers and Christensen studied relative stability of the Ba-IV structure against sc and sh in the pressure range from 100 to 200 GPa [12]. The Ba-IV structure is a kind of modulated structure. Despite these extensive studies, the structure of P-IV remains unidentified.

To explore the crystal structure of P-IV, we employed a metadynamics simulation with first-principles calculations. This trial was performed with a relatively small simulation cell to reduce the computational time. The simulation was designed, however, to be able to detect possible signals of structural phase transformations. We checked the relative stability of the structure obtained against the sc and sh phases. Next, we studied a number of model structures to find a more refined structure. A structural optimization was carried out for each model structure. The calculated x-ray powder patterns of the optimal structures were compared with that of the experimental structure.

In the metadynamics simulation, which was developed by Laio and Parrinello [13,14], we use the Gibbs free energy (GFE). GFE depends on the shape of the simulation cell. Following the formulation by Martoňák [14], we consider the GFE $G(\mathbf{h}^t) = G_o(\mathbf{h}^t) + G_g(\mathbf{h}^t)$, where $G_g(\mathbf{h}^t)$ is the artificial potential defined by the Gaussian-type function

$$G_g(\mathbf{h}^t) = \sum_{t'<t} \prod_{i,j} W \exp(-[\mathbf{h}^t - \mathbf{h}^{t'}]_{ij}^2/2\delta h^2). \quad (1)$$

The superscript t denotes the current metastep and t' the previous metastep. The quantities W and δh represent the weight and width of the Gaussian-type function, respectively. The matrix $\mathbf{h}$ is defined by $\mathbf{h} = (\vec{a}, \vec{b}, \vec{c})$, where $\vec{a}$, $\vec{b}$, and $\vec{c}$ are vectors defining the simulation cell. To eliminate the free rotation of the system, only the symmetric part of the matrix $\mathbf{h}$ is updated, whereby the number of independent variables to be updated in the simulation is reduced to 6.

The matrix $\mathbf{h}$ is updated by the steepest descent method by using the driving force $\mathbf{F}$ and taking δh as the stepping

parameter. $\mathbf{F}$ is obtained as the sum of the original driving force $\mathbf{F}_o = -\partial G_o/\partial \mathbf{h}$ and the Gaussian driving force $\mathbf{F}_g = -\partial G_g/\partial \mathbf{h}$. $\mathbf{F}_o$ can be expressed by an internal pressure tensor $\mathbf{p}$, external pressure P, and the matrix $\mathbf{h}$ [14]. Each step of updating $\mathbf{h}$ is defined as a metastep. At each metastep, in order to equilibrate the system and estimate $\mathbf{p}$, conventional molecular dynamics (MD) simulation steps must be run with the shape of the simulation cell fixed. The internal pressure tensor $\mathbf{p}$ and the atomic positions at each metastep can be obtained from the output of any constant-pressure MD code of the first-principles simulation, for which we used the PWSCF code [15]. If the current value of $\mathbf{h}$ is visited repeatedly, which occurs when the system fluctuates around the local minimum of the GFE surface, the artificial potential G_g attains a large value and the potential well is gradually filled with G_g.

For the simulation of phosphorus, we used density functional theory in a local density approximation and a norm-conserving pseudopotential, where we employed the expression by Perdew and Zunger [16] for the exchange-correlation energy functional. We checked the accuracy of our pseudopotential by comparing the calculated equation of states (EOS) with the experimental EOS for both the sc and the sh phase [8–10]. Calculated volume at 103 GPa for the sc phase is lower than the experimental value by 1.17%, and the volume at 151 GPa for the sh phase is lower by 2.33%.

We started the simulation with a cubic simulation cell whose edges were 4.26 Å, and the 8 phosphorus atoms in the cell were set at the positions that form the sc lattice. We performed the k-space integration using $8 \times 8 \times 8$ mesh points in the first Brillouin zone and set the energy cutoff of the plane wave basis at 40 Ry. We also set the external pressure to 120 GPa in the conventional constant-pressure MD since the P-IV phase is observed around this pressure. In order to equilibrate the system, we ran the MD simulation for 200 steps for each metastep and calculated the average internal pressure tensor from the latter half consisting of 100 steps. We used cluster machines with 16–32 nodes to perform this metadynamics simulation.

Figure 1 shows the evolution of the cell volume and the three angles between the vectors defining the simulation cell. We started the simulation with the Gaussian potential off by setting $W = 0$ mRy for 38 metasteps to check whether the sc structure was stable. During these initial metasteps, the values of the angles and the volume of the sc lattice were nearly maintained. This means that the sc structure resides at a local minimum and is well separated from the other local minima by certain potential barriers. We note that the metadynamics simulation with the Gaussian-type potential switched off is nearly equivalent to the conventional variable-cell MD simulations.

To explore the structures beyond the potential barrier, we switched the Gaussian-type potential on at the 39th metastep by setting the W to 1 mRy and δh to 20 mÅ. As a result, one of the three angles started to increase at around

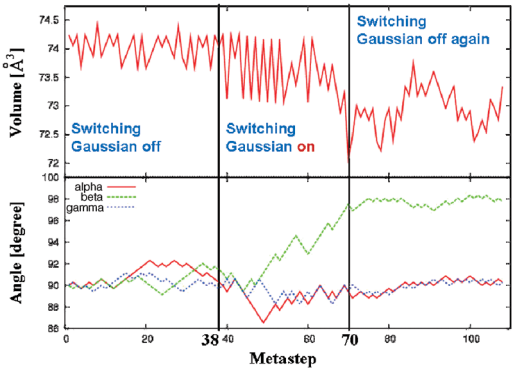

FIG. 1 (color online). Evolution of the simulation cell volume and the angles between the cell vectors. The Gaussian-type potential is switched off during the first 38 metasteps, switched on at the 39th metastep, and off again after the 71st metastep.

the 50th metastep and the volume began to decrease dramatically. After those changes, we switched the Gaussian-type potential off at the 71st metastep again to check whether the system had surmounted the potential barrier and moved to a neighboring local minimum. If the system had not crossed the barrier yet, the angle and the volume would have returned to the starting values of the sc lattice, which are approximately 90° and 74 Å^3, respectively. After the 71th metastep, however, the volume fluctuated around 73 Å^3 and the three angles also continued to fluctuate around 90°, 98°, and 90°. This behavior shows that the sc structure transformed into another metastable structure.

Figure 2 shows the structure obtained by the above metadynamics run. This structure has a simulation cell with the following cell parameters: $a = 4.22$ Å, $b = 4.15$ Å, $c = 4.22$ Å, $\alpha = 90.86°$, $\beta = 97.76°$, and $\gamma = 90.26°$. The figure on the left-hand side is a projection onto the ac plane. It shows the distortion from the cubic to the monoclinic unit cell through an angle of 97.76°. When we view the lattice from the side, we find a zigzag modulation pattern of the ac plane along the b axis with a displacement in the [101] direction, as shown by the $ABAB\ldots$ planes in the figure on the right-hand side. The $ABAB\ldots$ modulation

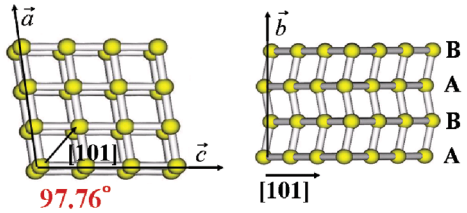

FIG. 2 (color online). A structure obtained by the first-principles metadynamics simulation. $\vec{a}$, $\vec{b}$, and $\vec{c}$ are vectors defining the simulation cell, and $a = 4.22$ Å, $b = 4.15$ Å, $c = 4.22$ Å, $\alpha = 90.86°$, $\beta = 97.76°$, and $\gamma = 90.26°$. It is seen that the ac planes along the b axis are displaced in an alternating fashion in the [101] direction.

pattern is crucial for the stability of the monoclinic distortion of the unit cell. When we performed the simulation by suppressing the zigzag modulation pattern while allowing the relaxation of the shape of the simulation cell, we observed that the structure returned to the initial sc structure.

The structure obtained by the metadynamics simulation is a modulated structure with a period consisting of two planes, namely, $ABAB\ldots$. Our simulation, however, was performed using a system with 8 atoms in the simulation cell and with a periodic boundary condition. Hence, there remains the question of whether the small simulation cell and the periodic boundary condition may limit the modulation period to a shorter period. Indeed, in the x-ray powder pattern of the obtained structure, apparently three or four minor peaks are not observed in the experimental pattern, although most of the main peaks agree with the peaks of the experimental pattern. To answer this question, we extended our study to include several other structures by increasing the modulation period.

We carried out first-principles calculations of the total energy for two more structures with commensurate modulations: a structure with an $ABAC\ldots$ type stacking of planes and one with an $ABCBADED\ldots$ type pattern. The modulation periods of the $ABAC\ldots$ and $ABCBADED\ldots$ type structures are, respectively, twice and 4 times as long as that of the $ABAB\ldots$ type. These structures, denoted by M4 and M8, respectively, are shown in Fig. 3 along with M1, which is a nonmodulated structure, and M2, the structure obtained by the metadynamics simulation.

To compare the total energy among these structures, we used the same unit cell with the lattice vectors $\vec{a}/2$, $4\vec{b}$, and $\vec{c}/2$, where $\vec{a}$, $\vec{b}$, and $\vec{c}$ are those obtained by the metadynamics simulation. The eight atoms were set along the b axis in the unit cell with displacements corresponding to the modulation pattern (Fig. 3). This choice of the unit cell avoids numerical errors due to the use of structures having different sized unit cells. For the k-space integration, we used $16 \times 4 \times 16$ mesh points in the first Brillouin zone. We checked the stability of the M2, M4, and M8 structures by relaxing the atomic positions. Each structure was stable around atomic positions corresponding to the respective modulation pattern. We obtained the total energy for these structures by fully optimizing the atomic positions. The results are listed in Table I. All modulated structures, namely, M2, M4, and M8, have lower energies than the nonmodulated structure M1. Among the modulated structures, M4 has the lowest energy.

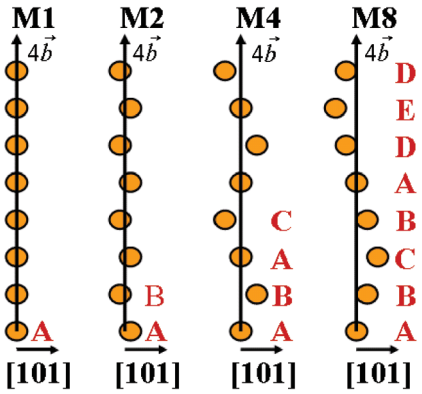

FIG. 3 (color online). Modulated structures with different modulation periods along the b axis. Pattern M1 is of a nonmodulated structure, and M2 is the structure obtained by our metadynamics simulation ($ABAB\ldots$). The modulation periods of M4 ($ABAC\ldots$) and M8 ($ABCBADED\ldots$) patterns are twice and 4 times as long as that of M2, respectively.

To estimate the stable pressure region of the M4 structure, we calculated the enthalpy of the M4 phase. According to our results, the enthalpy of M4 is lower than those of the sc and sh structures in the pressure range from 118 to 128 GPa. The P-IV phase is experimentally observed from 107 to 137 GPa. The discrepancy between our stable region and that obtained experimentally is presumably attributable to the commensurate approximation we used in the present study. We should mention here that the enthalpy of all the structures proposed by Ehlers and Christensen [12] lay above the enthalpy of the sh over the entire pressure range.

In Fig. 4, we compare the x-ray powder patterns of our structures with the experimental pattern. The experimental pattern of P-IV (top figure) was obtained from Akahama *et al.*'s [8]. We note the split in the strongest peak at $2\theta = 13°$ and the three peaks in the range from $2\theta = 17°$ to $19°$. These features are missing in our M2 structure. Instead, superfluous peaks are observed at $2\theta = 15°$ and $25°$. However, these discrepancies are eliminated in structures with longer modulation periods. The intensities of the superfluous peaks that appeared in the M2 structure at $2\theta = 15°$ (due to the zigzag modulation) and $2\theta = 25°$ (due to the distortion of the simulation cell from a cubic structure) both decreased in the M4 and M8 structures. The strongest peak split in both M4 and M8. As for the intensity of the three peaks in the range from $2\theta = 17°$ to $19°$, the x-ray powder pattern of M4 showed the best agreement with the experimental pattern among the 4 patterns studied. On the basis of a comparison of the total energies and x-ray

TABLE I. Comparison of the total energies per atom for the nonmodulated structure (M1) and the three modulated structures (M2, M4, and M8). We used the unit cell with the lattice vectors $\vec{a}/2$, $4\vec{b}$, and $\vec{c}/2$ in calculating the total energy for all of these four structures, where $\vec{a}/2$, $4\vec{b}$, and $\vec{c}/2$ were obtained by the metadynamics simulation.

Structure	Total energy [Ry/atom]
M1	−13.1624
M2	−13.1638
M4	−13.1642
M8	−13.1637

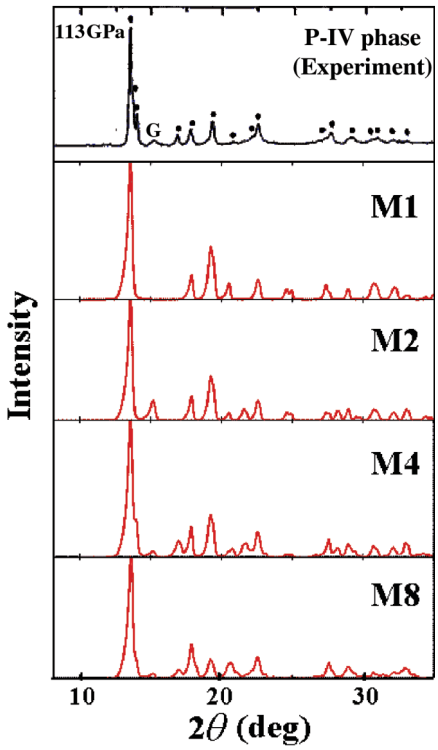

FIG. 4 (color online). Comparison of the experimental x-ray powder pattern of the P-IV [8] phase with those of the modulated structures M1, M2, M4, and M8. Theoretical powder patterns of the modulated structures are obtained by using RIETAN-2000 [17]. In the experimental pattern, Akahama *et al.* [8] indicated observed peaks by dots and the peak due to the metal gasket by the letter *G*.

powder patterns, we conclude that the structure of the P-IV closely resembles the M4 structure or an incommensurately modulated structure with a modulation period very close to that of M4.

In this study, we explored the structure of phosphorus in phase IV using a first-principles metadynamics simulation and identified the new structure. The structure is monoclinic with a modulated pattern. Furthermore, we have found the refined structure showing the best agreement with the x-ray powder pattern. Although we have not fully studied the possibility of incommensurate modulation, we conclude that phosphorus takes on a modulated structure with possible incommensurate modulation. The hypothesis by Akahama *et al.* [8] that the structure of P-IV may be on the path from sc to sh via monoclinic distortion along the [101] direction is partially supported because the unmodulated structure is of space group $P2$ and has one atom per unit cell. The modulation stabilizes the monoclinic distortion of the lattice from the simple cubic structure. It is highly probable that Vb, VIb, and VIIb group elements commonly show modulated structures in a narrow pressure range between simple stable structures when they undergo pressure-induced structural transformations.

The authors thank Dr. Nakamoto and Dr. Morimoto for valuable discussions on the x-ray powder patterns. Computations were performed at the Institute for Molecular Science, Okazaki, Aichi, Japan. This work was partially supported by a Grant-in-Aid for Scientific Research in Priority Areas "Development of New Quantum Simulators and Quantum Design" (No. 17064006 and No. 17064013) and by Grants-in-Aid for Scientific Research (No. 15GS0123 and No. 15310086) and a Computational Nanoscience program "Grid Application Research in Nanoscience-National Research Grid Initiative (NAREGI)" of The Ministry of Education, Culture, Sports, Science, and Technology, Japan. Additional support was provided by NEDO under the Nanotechnology Materials Program.

*Electronic address: ishikawa@aquarius.mp.es.osaka-u.ac.jp
†Electronic address: nagara@mp.es.osaka-u.ac.jp
‡Electronic address: kabe@mp.es.osaka-u.ac.jp
§Electronic address: suzuki@mp.es.osaka-u.ac.jp

[1] M. I. McMahon, O. Degtyareva, and R. J. Nelmes, Phys. Rev. Lett. **85**, 4896 (2000).
[2] U. Shwartz, L. Akselrud, H. Rosner, A. Ormeci, Y. Grin, and M. Hanfland, Phys. Rev. B **67**, 214101 (2003).
[3] C. Hejny, L. F. Lundegaard, S. Falconi, and M. I. McMahon, Phys. Rev. B **71**, 020101 (2005).
[4] M. I. McMahon, C. Hejny, J. S. Loveday, and L. F. Lundegaard, Phys. Rev. B **70**, 054101 (2004).
[5] C. Hejny and M. I. McMahon, Phys. Rev. Lett. **91**, 215502 (2003).
[6] K. Takemura, K. Sato, H. Fujihisa, and M. Onoda, Nature (London) **423**, 971 (2003).
[7] T. Kume, T. Hiraoka, Y. Ohya, S. Sasaki, and H. Shimizu, Phys. Rev. Lett. **94**, 065506 (2005).
[8] Y. Akahama, M. Kobayashi, and H. Kawamura, Phys. Rev. B **59**, 8520 (1999).
[9] I. Hamada, T. Oda, and N. Suzuki, *Science and Technology of High Pressure, Proceedings of AIRAPT-17* (University Press, Delhi, India, 2000), Vol. 1, p. 467.
[10] Y. Akahama and H. Kawamura, Phys. Rev. B **61**, 3139 (2000).
[11] R. Ahuja, Phys. Status Solidi B **235**, 282 (2003).
[12] F. J. H. Ehlers and N. E. Christensen, Phys. Rev. B **69**, 214112 (2004).
[13] A. Laio and M. Parrinello, Proc. Natl. Acad. Sci. U.S.A. **99**, 12 562 (2002).
[14] R. Martoňák, A. Laio, and M. Parrinello, Phys. Rev. Lett. **90**, 075503 (2003).
[15] S. Baroni, A. D. Corso, S. de Gironcoli, and P. Giannozzi, The PWSCF code is available through: http://www.pwscf.org/.
[16] J. P. Perdew and A. Zunger, Phys. Rev. B **23**, 5048 (1981).
[17] F. Izumi and T. Ikeda, Mater. Sci. Forum **321**, 198 (2000).